Dust Properties of Powerful Radio Galaxies

From Dust to Galaxies

IAP - 29th June 2011

Jason Rawlings

Nicholas Seymour, Mat Page, Myrto Symeonidis (MSSL, UCL)

Outline

- High redshift radio galaxies
- Mid-IR diagnostics
- PAHs
- PAHs as a star formation tracer
- Previous spectroscopy
- Aims
- Samples
- Spectral fitting
- Results & Conclusions

High Redshift Radio Galaxies (HzRGs)

- Radio loud AGN, $L_{3GHz} > 10^{24}$ WHz^{-1}, $z > 1$
- Massive stellar hosts (~5 x $10^{11} M_{sun}$) (Seymour et al. 2007)
- Very powerful AGN with high accretion rates (Ogle et al. 2006; Seymour et al. 2007)
- Some have strong sub-mm emission (Archibald et al. 2001; Reuland et al. 2004; Greve et al. 2006)- lots of cold dust
- Very short time scales for jets and star formation (<0.1Gyr)

  - Implies special phase of coeval black hole and galaxy growth

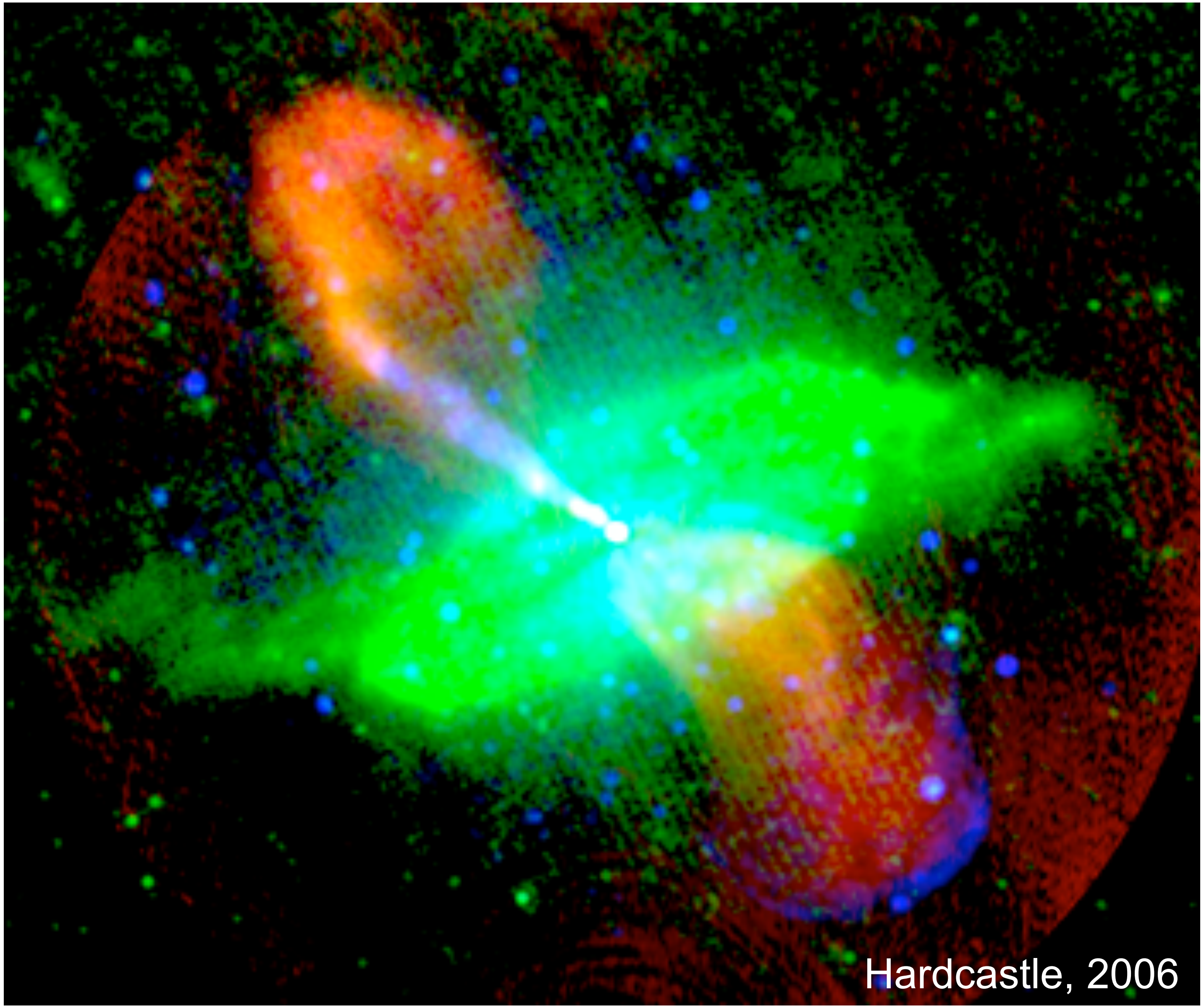
Hardcastle, 2006

Mid-IR diagnostics

- HzRGs hosts
- Can star formation be associated with powerful, obscured AGN? At high redshift?
- Mid-IR emission allows studies of both AGN and host properties
- Mid-IR continuum due to dust in the torus- tracer of AGN power
- Mid-IR PAH emission: approximate measure of SFR
- SFR diagnostics at non-IR wavelengths can be contaminated by the AGN

Polycyclic Aromatic Hydrocarbons (PAHs)

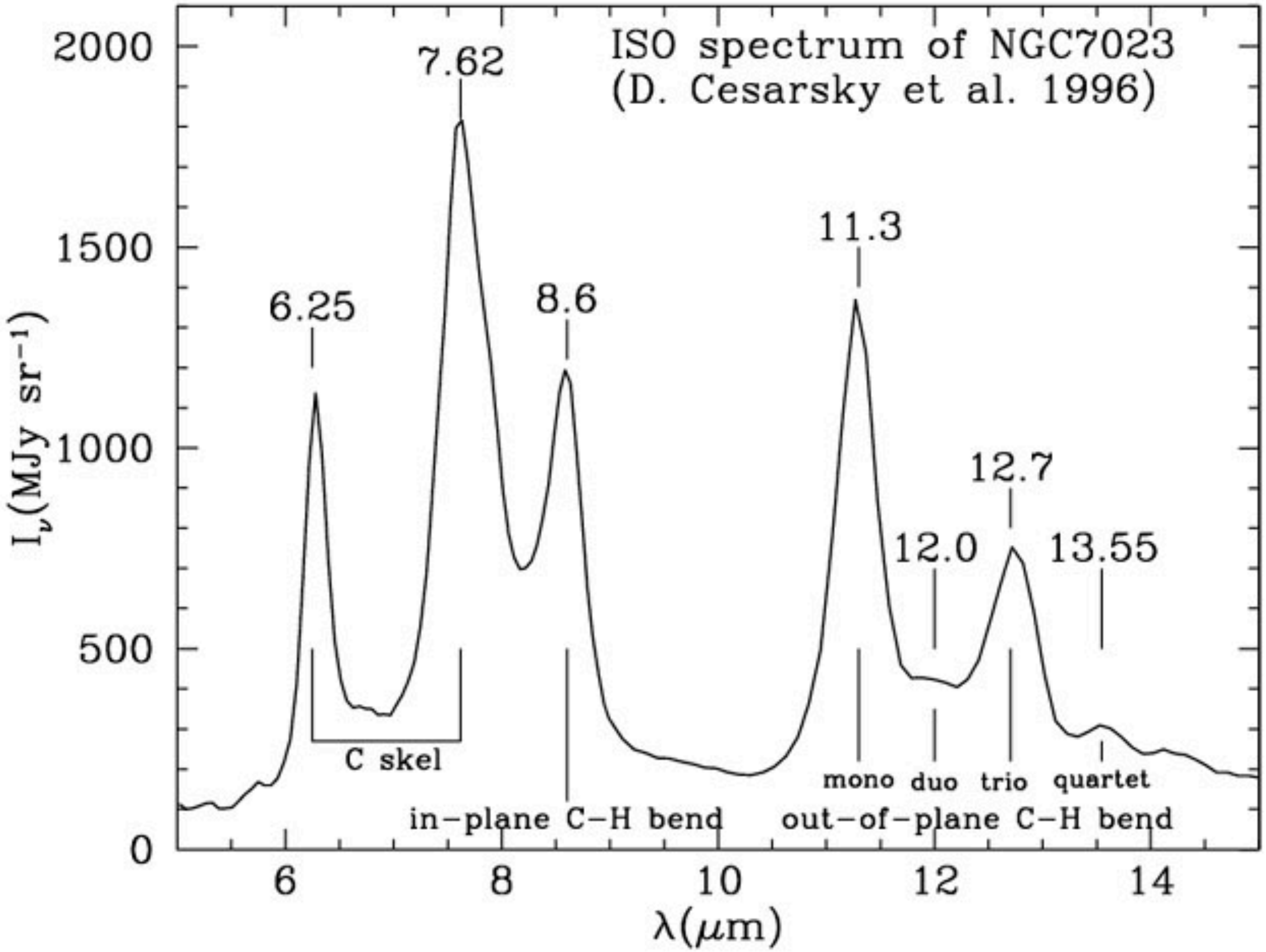

PAH emission as a SF tracer

- PAH - sub-mm luminosity correlation found in local starbursts (Haas et al. 2002; Peeters et al. 2004)
- PAH emission linked to cold dust associated with SF (Lacy et al. 2007; Pope et al. 2007; Sajina et al. 2008)
- Weak PAH emission in lower redshift radio galaxies. What about higher redshift?

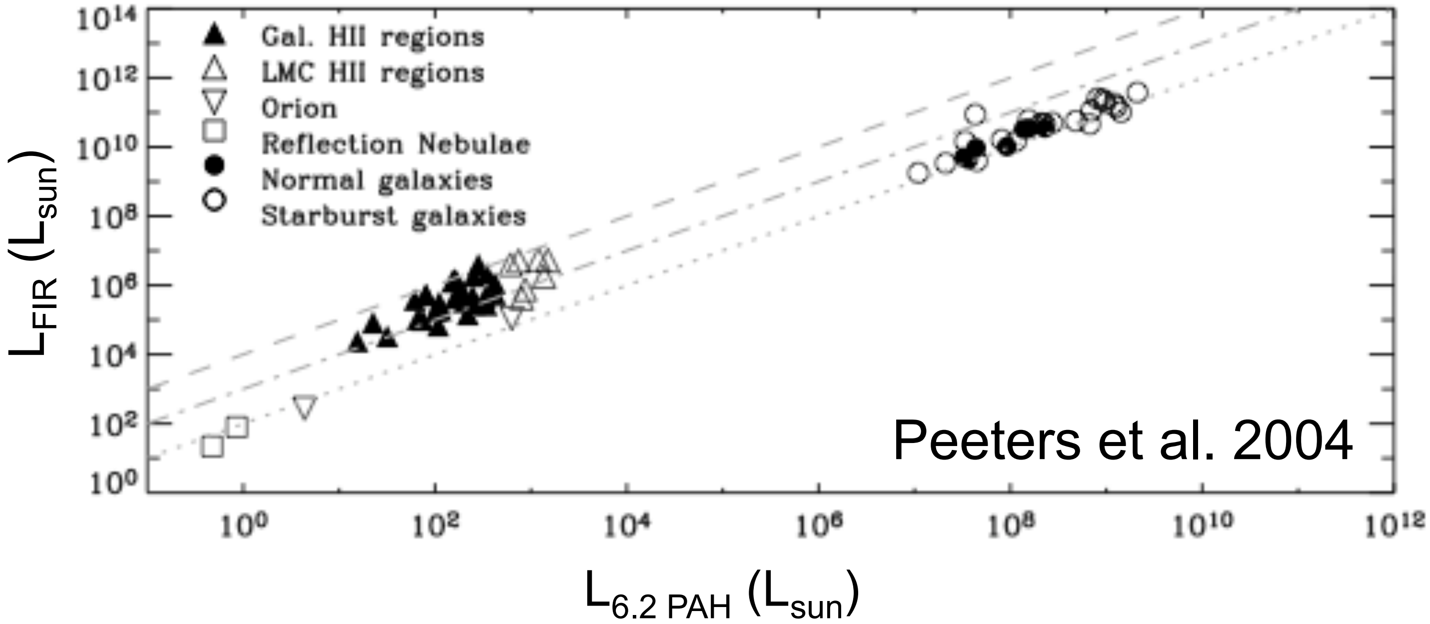

Previous spectroscopy of HzRGs

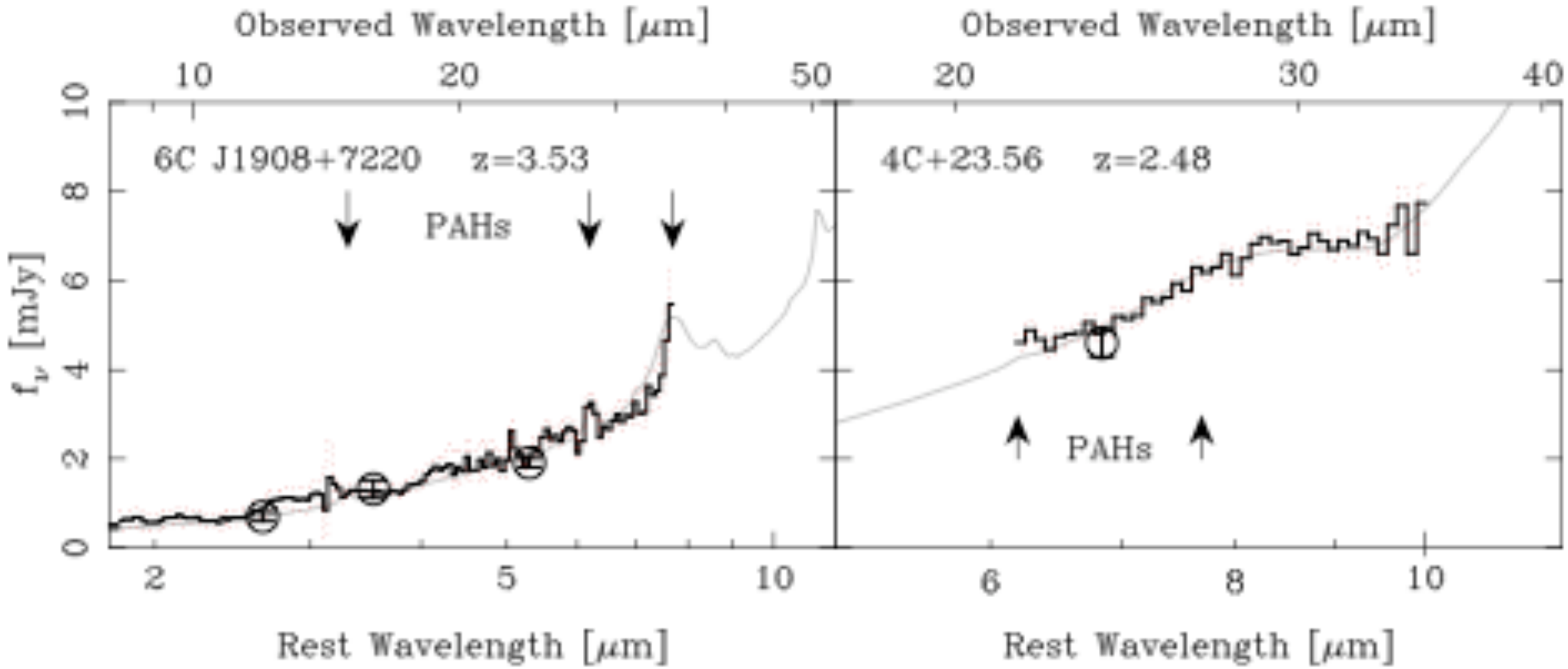

Seymour et al. 2008

- Full IR SED fitting for 2 HzRGs
- L_{500MHz}: 7.9x10^{28}, 1.3x10^{29} (ergs s^{-1} Hz^{-1})
- SFRs: 4000 ± 700, ≤100 (M_{sun} yr^{-1}), $\tau_{9.7\mu m}$: 0.3 ±0.05

Spitzer- InfraRed Spectrograph (IRS)

- High resolution (R~ 600): 10-20 µm (SH), 19-37 µm (LH)
- Low resolution (R~ 60-120): 5-14 µm (SL), 14-40 µm (LL)

- z < 3.5; PAH emission, Si absorption (~9.7 µm)

Flux density distribution for the 24µm population in the ELAIS-N1

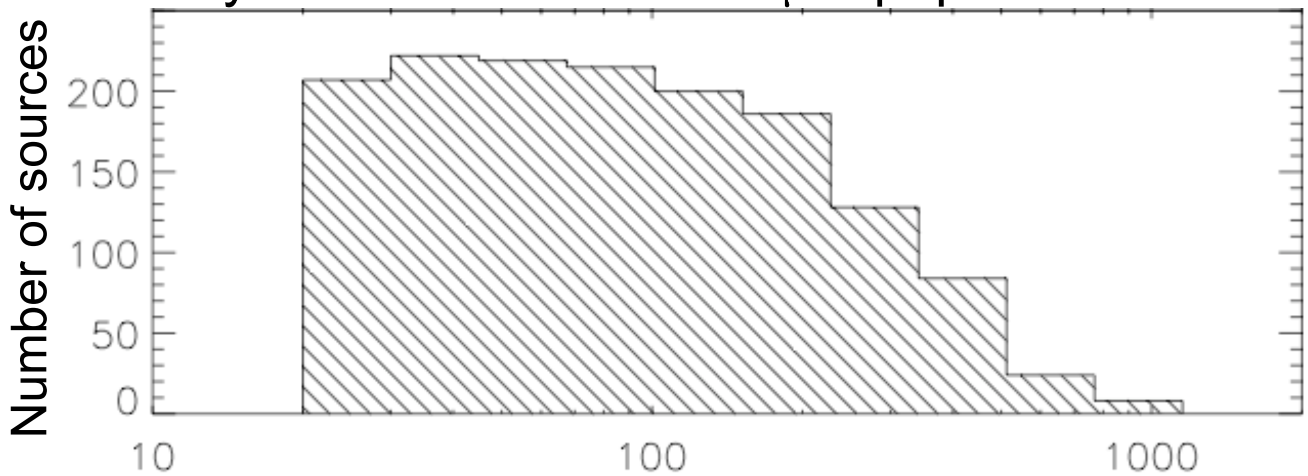

F_ν (24µm) [µJy]

Chary et al. 2004

Spitzer- InfraRed Spectrograph (IRS)

- High resolution (R~ 600): 10-20 μm (SH), 19-37 μm (LH)
- Low resolution (R~ 60-120): 5-14 μm (SL), 14-40 μm (LL)

- z < 3.5; PAH emission, Si absorption (~9.7 μm)

Flux density distribution for the 24μm population in the ELAIS-N1

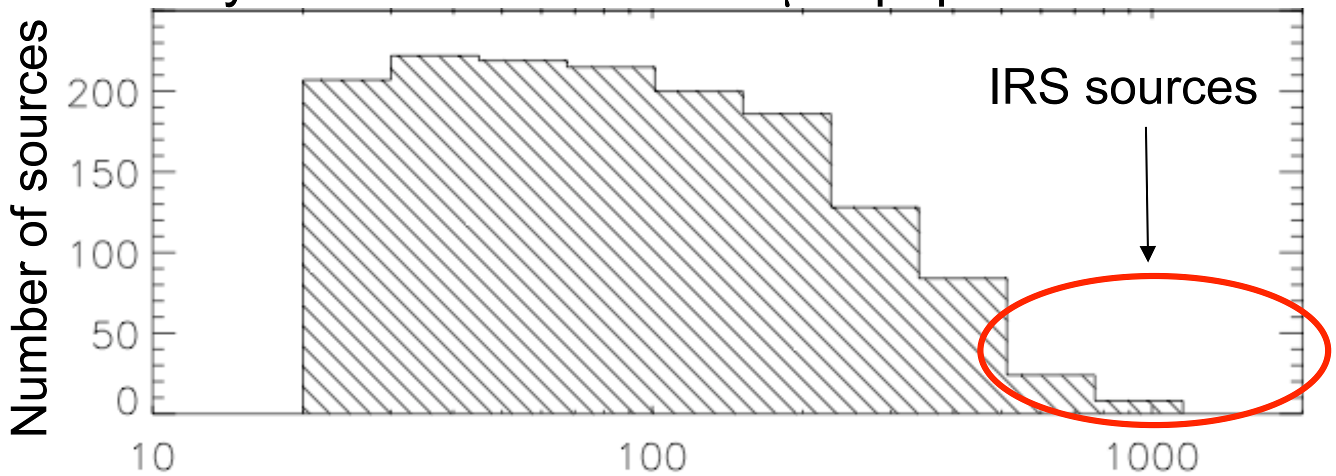

F_ν (24μm) [μJy]

Chary et al. 2004

Aims

- Using *Spitzer*-IRS LL data to perform spectroscopy on HzRGs ($1.5 < z < 3.2$)
- To measure PAH emission, silicate absorption features and underlying continua (at 5-13 μm)
- To estimate SFRs, accretion power and obscuration of the AGN

The samples:

- High radio luminosity
  - $L_{3GHz} = 10^{27-28}$ WHz^{-1}
  - Spitzer High redshift Radio Galaxy (SHzRG) survey (Seymour et al. 2007)

- Moderate radio luminosity
  - $L_{3GHz} = 10^{25-26}$ WHz^{-1}
  - Boötes Field

Distribution of 24μm flux densities

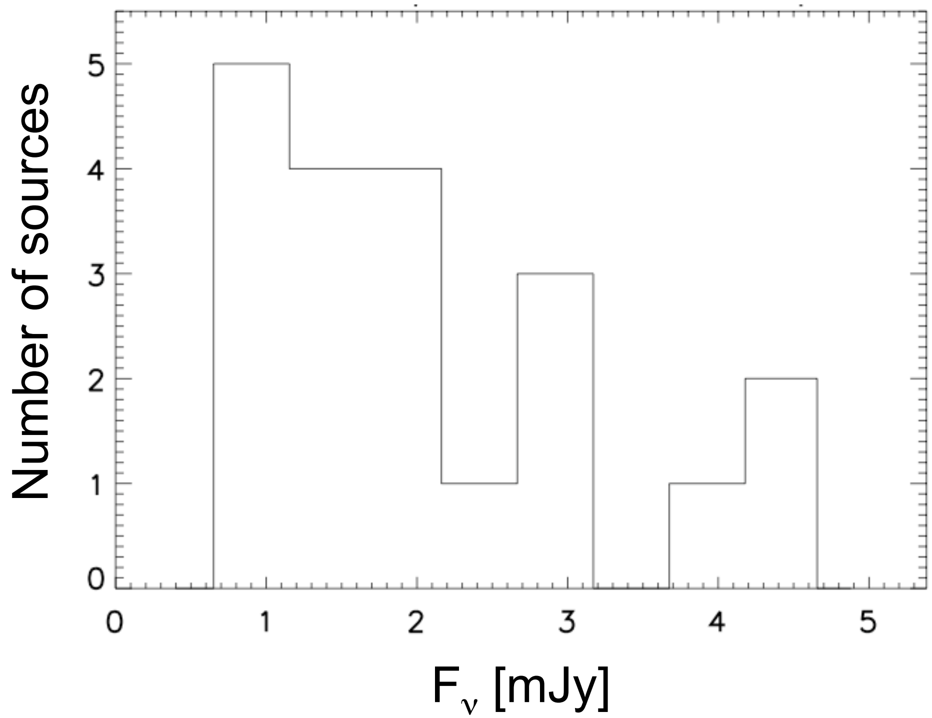

- Lower radio luminosity ($L_{3GHz} = 10^{24-25}$ WHz^{-1}); First Look Field (Yan et al. 2007) selection criteria:

  $S_{24\mu m}$ > ~1mJy, $S_{24\mu m}$>> $S_{R\text{-band}}$ (dusty))

Spectral fitting

- Brandl et al. 2006 local starburst (SB) IRS spectra used as templates to model SB component.
- Power law used to represent AGN component.
- Components normalised and extinction corrected, χ^2 minimisation performed for each template.
- From each best fit, the separate contributions of the SB and AGN components can be deduced.

Individual spectra

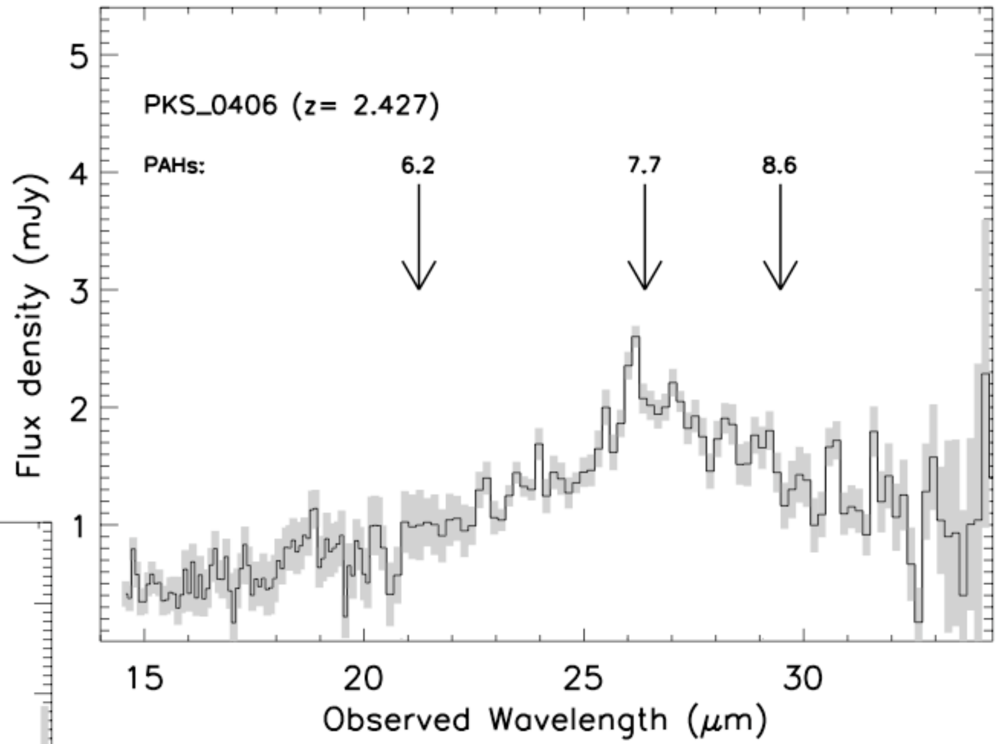

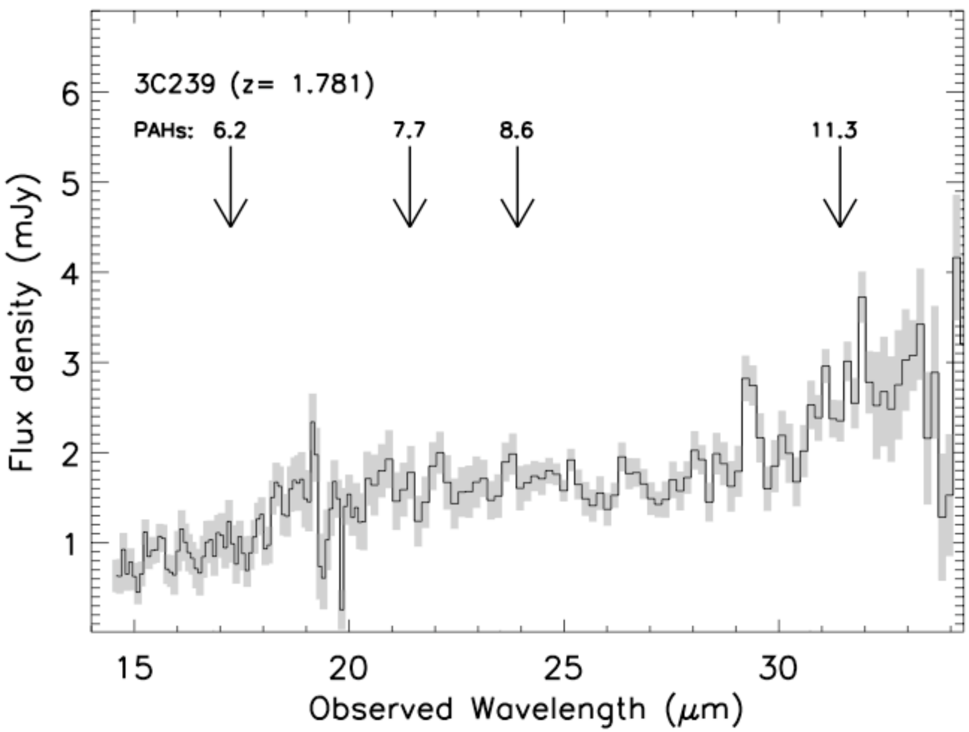

Individual spectra

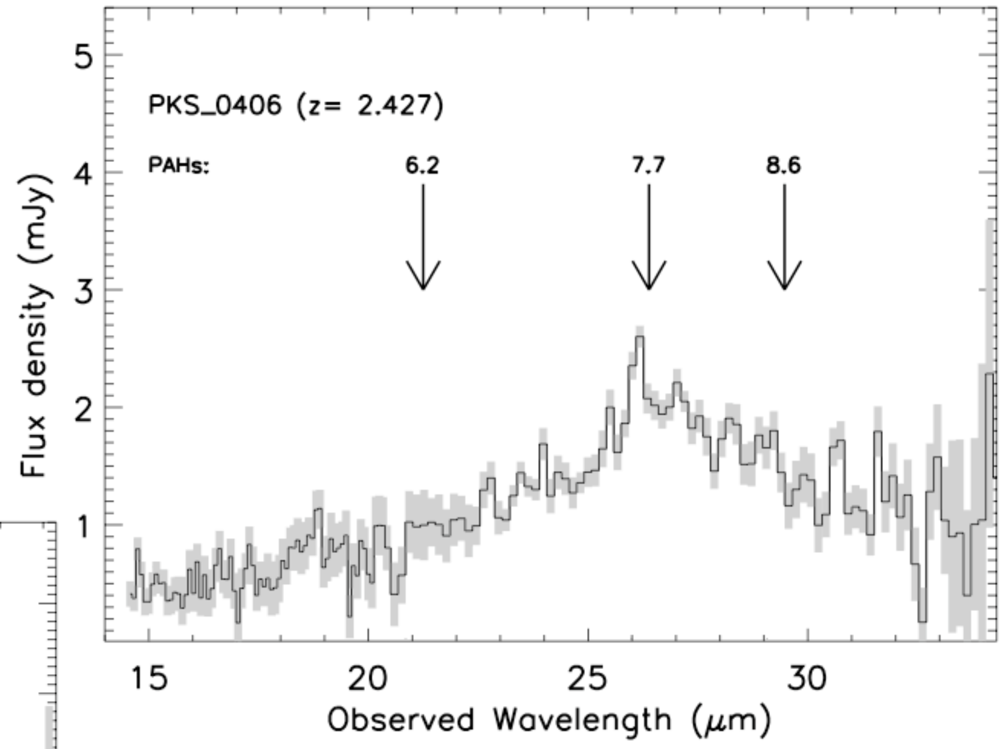

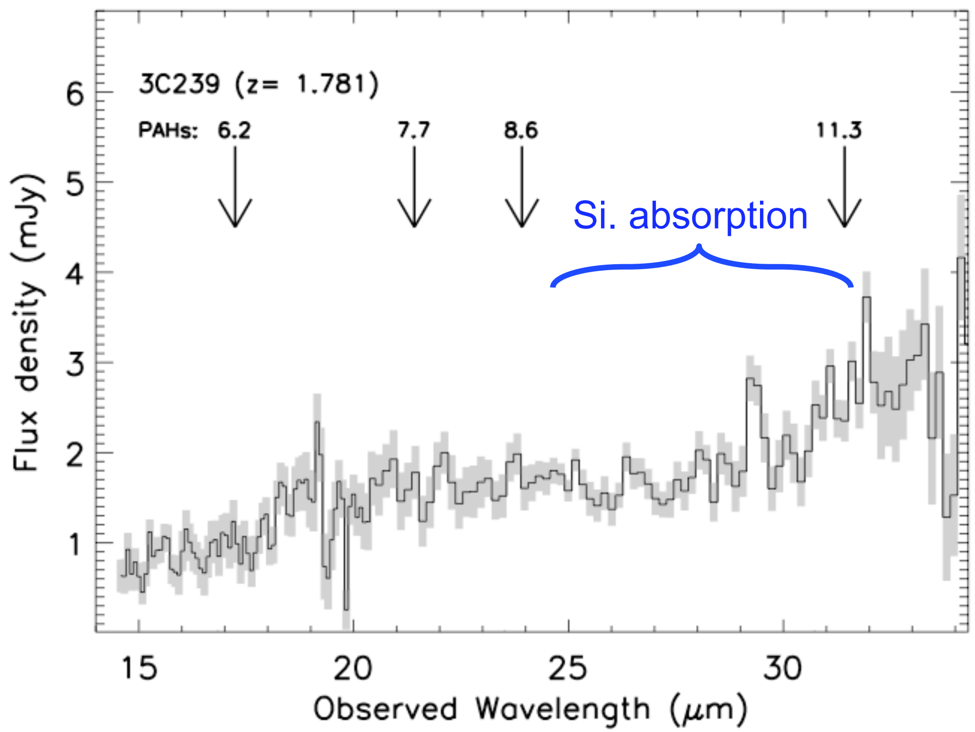

Individual spectra

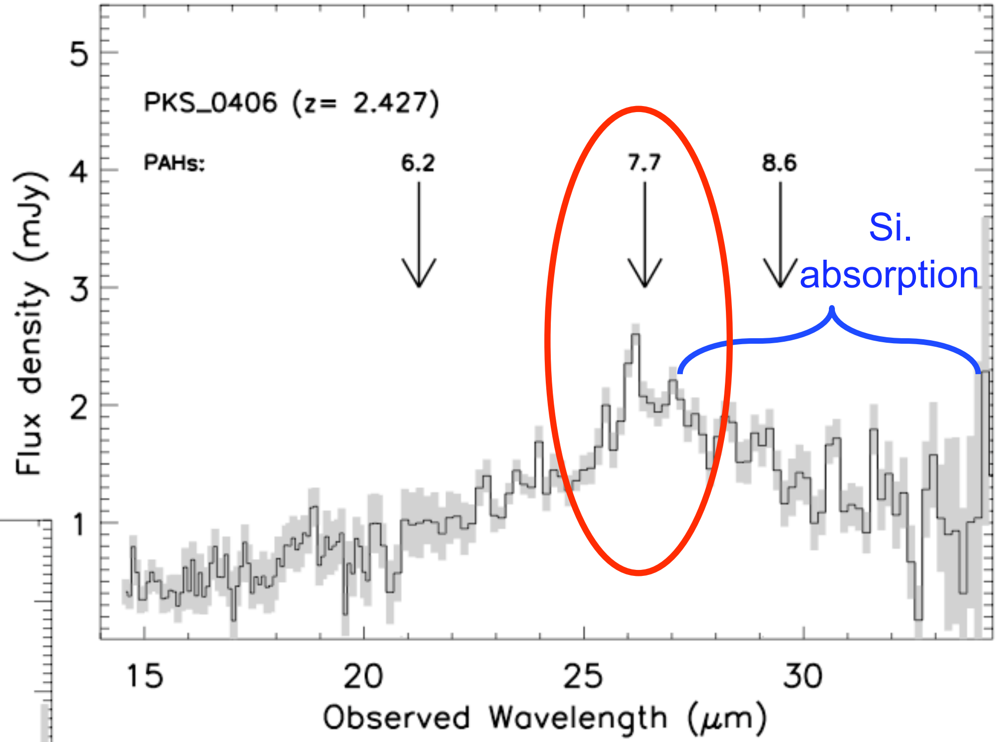

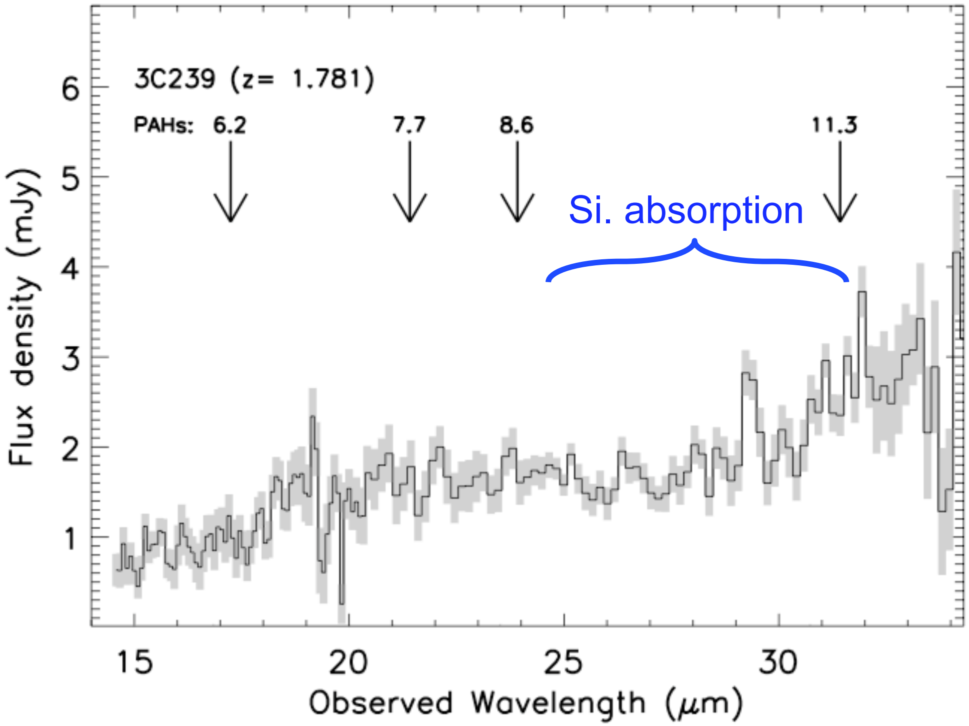

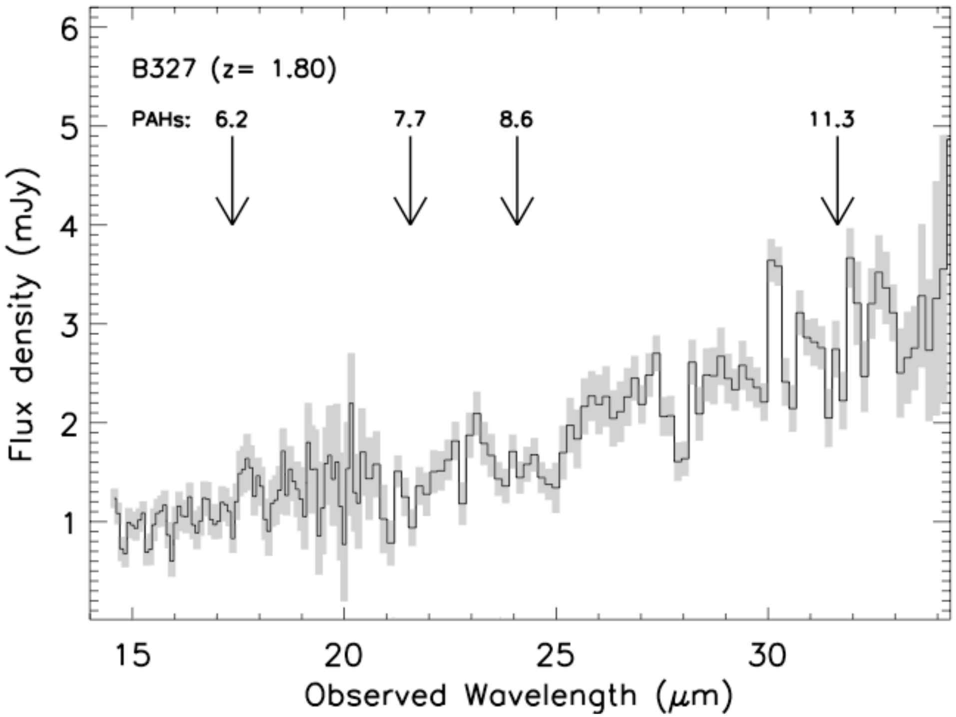
B327 (z= 1.80)
PAHs: 6.2 7.7 8.6 11.3
Flux density (mJy)
Observed Wavelength (μm)

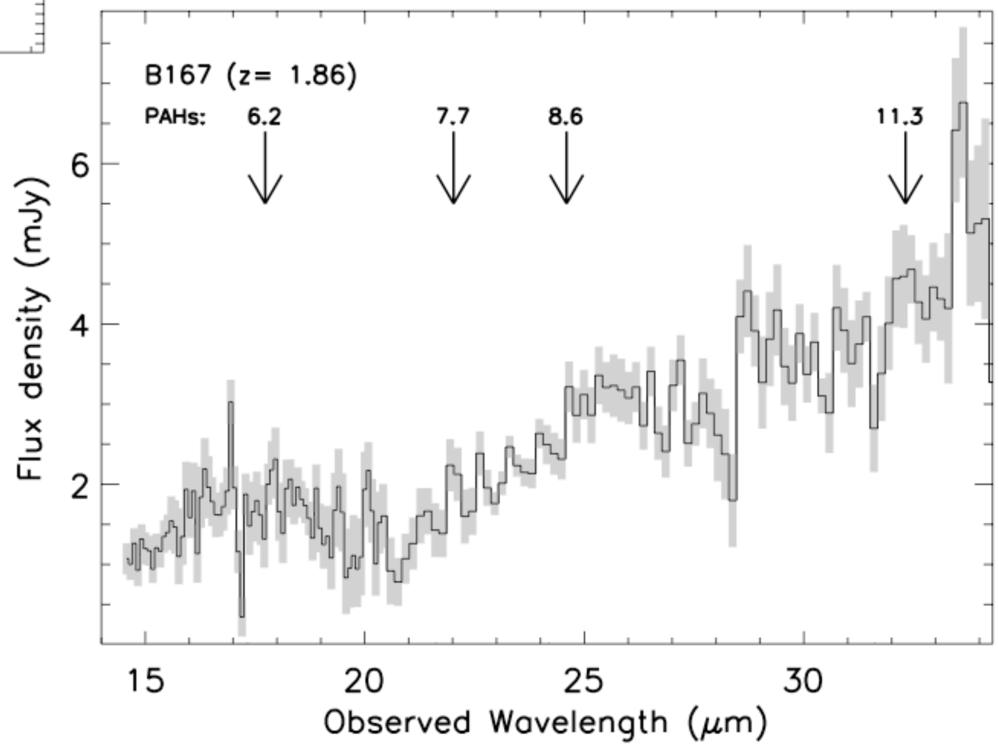
B167 (z= 1.86)
PAHs: 6.2 7.7 8.6 11.3
Flux density (mJy)
Observed Wavelength (μm)

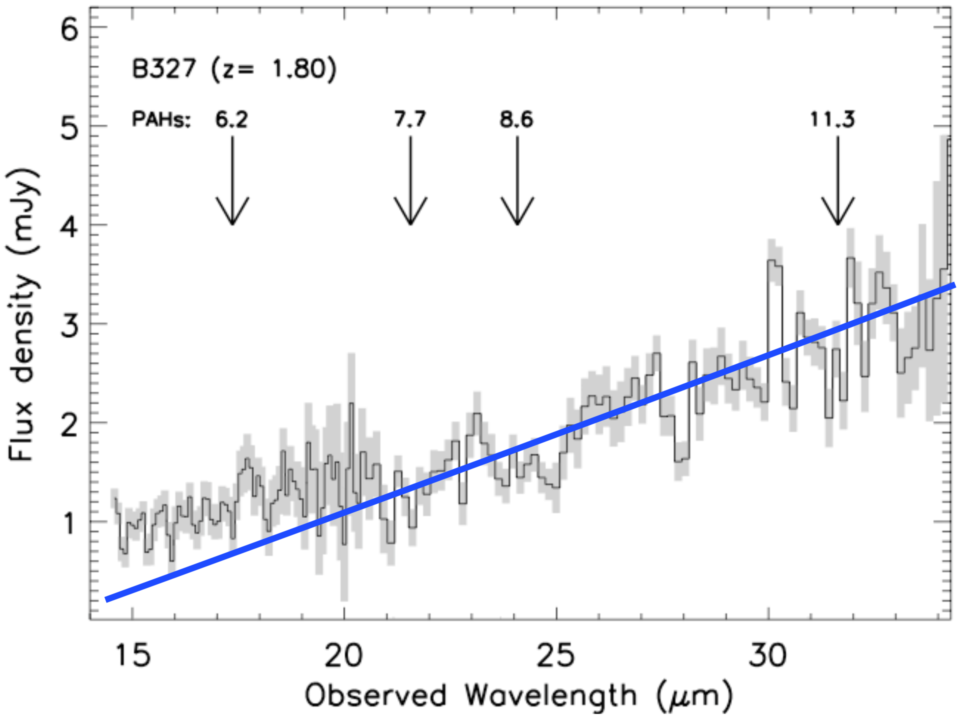
B327 (z= 1.80)
PAHs: 6.2
7.7
8.6
11.3
Flux density (mJy)
Observed Wavelength (μm)

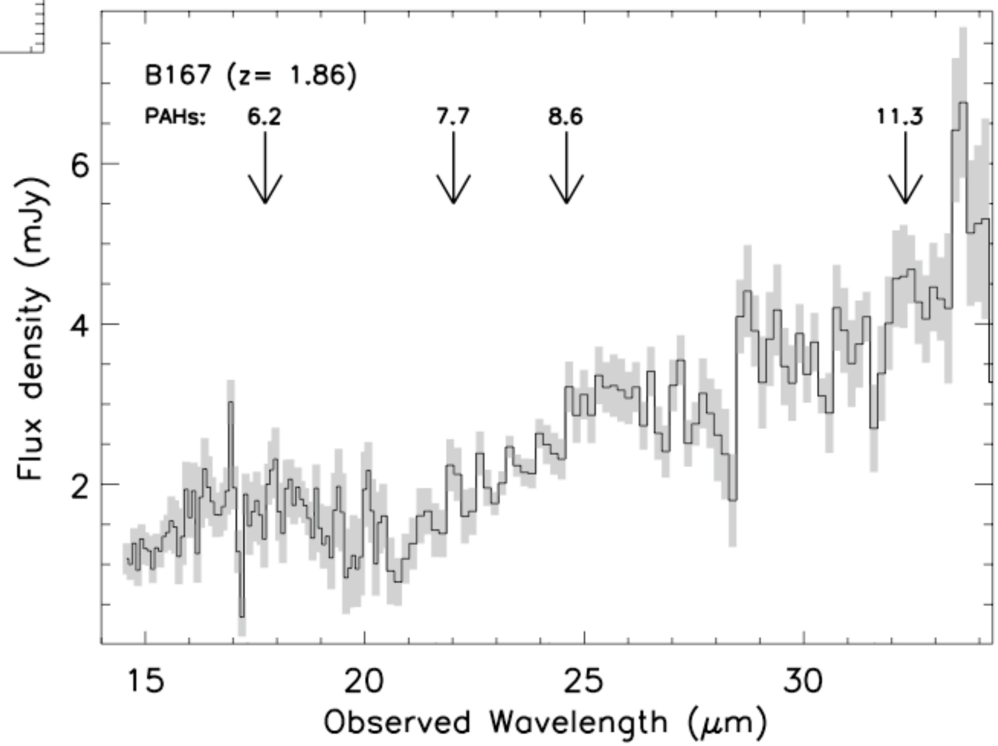
B167 (z= 1.86)
PAHs: 6.2
7.7
8.6
11.3
Flux density (mJy)
Observed Wavelength (μm)

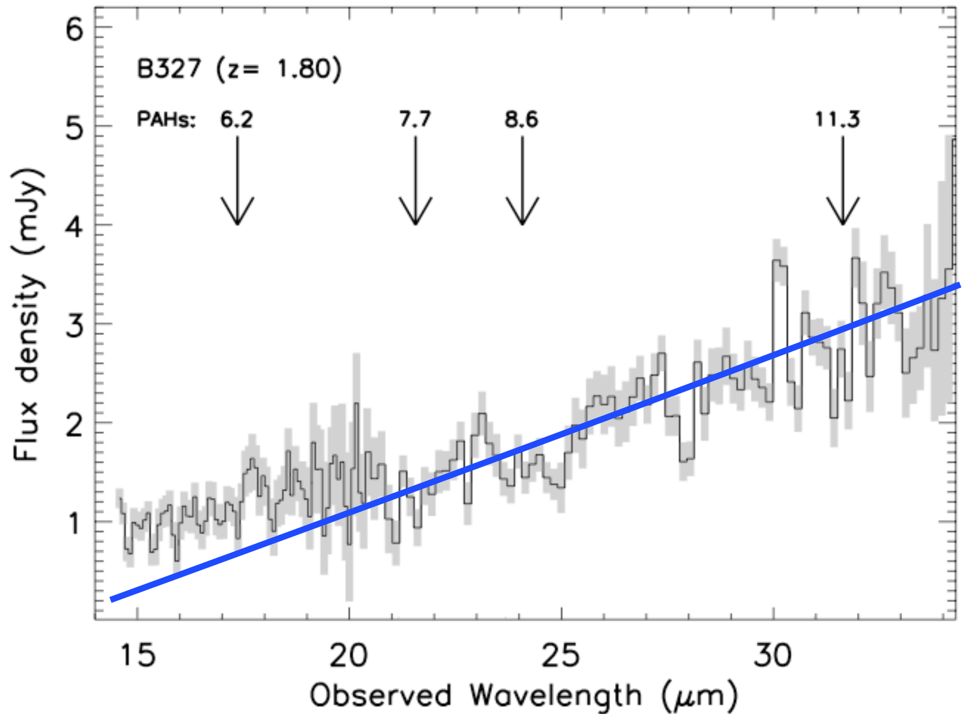
B327 (z= 1.80)
PAHs: 6.2
7.7
8.6
11.3
Flux density (mJy)
Observed Wavelength (μm)
15
20
25
30
1
2
3
4
5
6

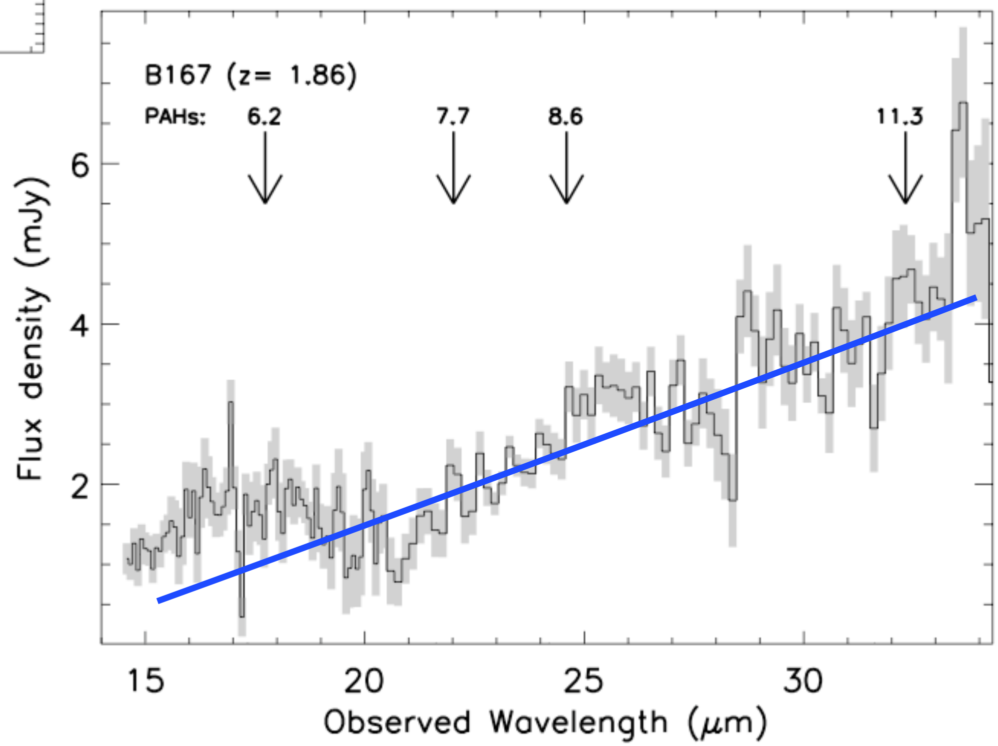
B167 (z= 1.86)
PAHs: 6.2
7.7
8.6
11.3
Flux density (mJy)
Observed Wavelength (μm)
15
20
25
30
2
4
6

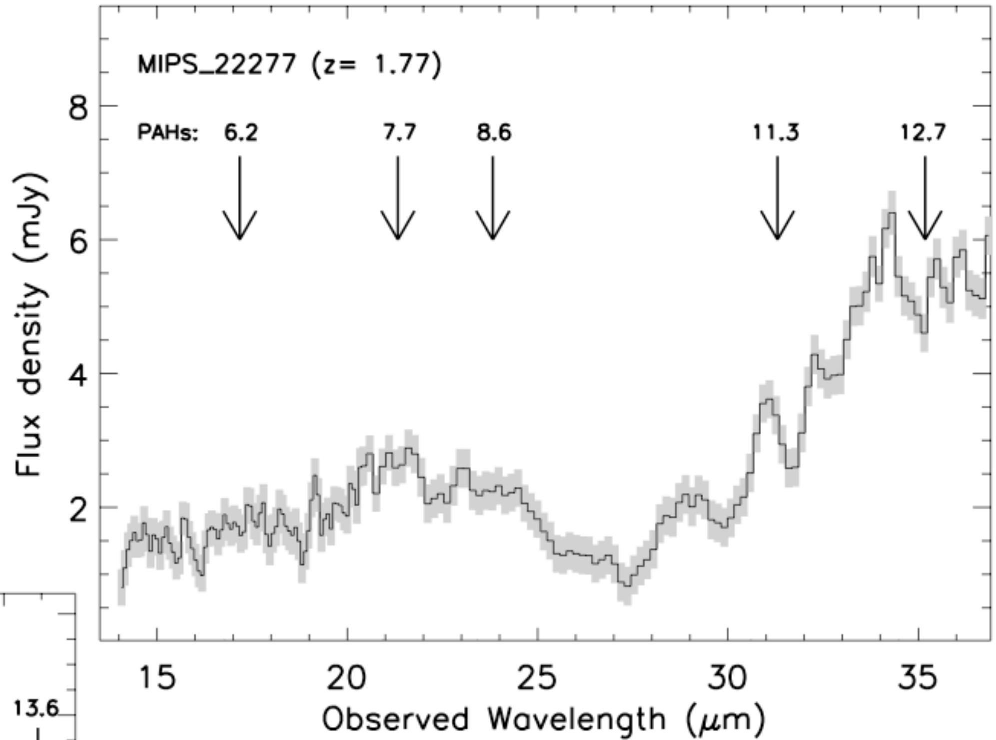
MIPS_22277 (z= 1.77)
PAHs: 6.2 7.7 8.6 11.3 12.7
Flux density (mJy)
Observed Wavelength (μm)

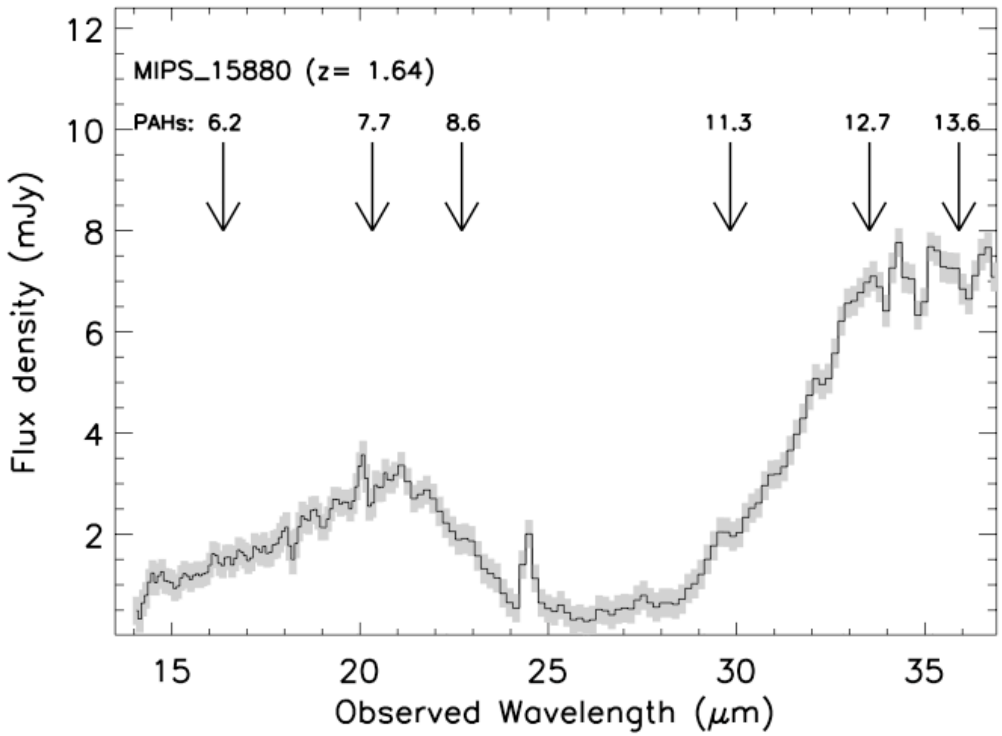
MIPS_15880 (z= 1.64)
PAHs: 6.2 7.7 8.6 11.3 12.7 13.6
Flux density (mJy)
Observed Wavelength (μm)

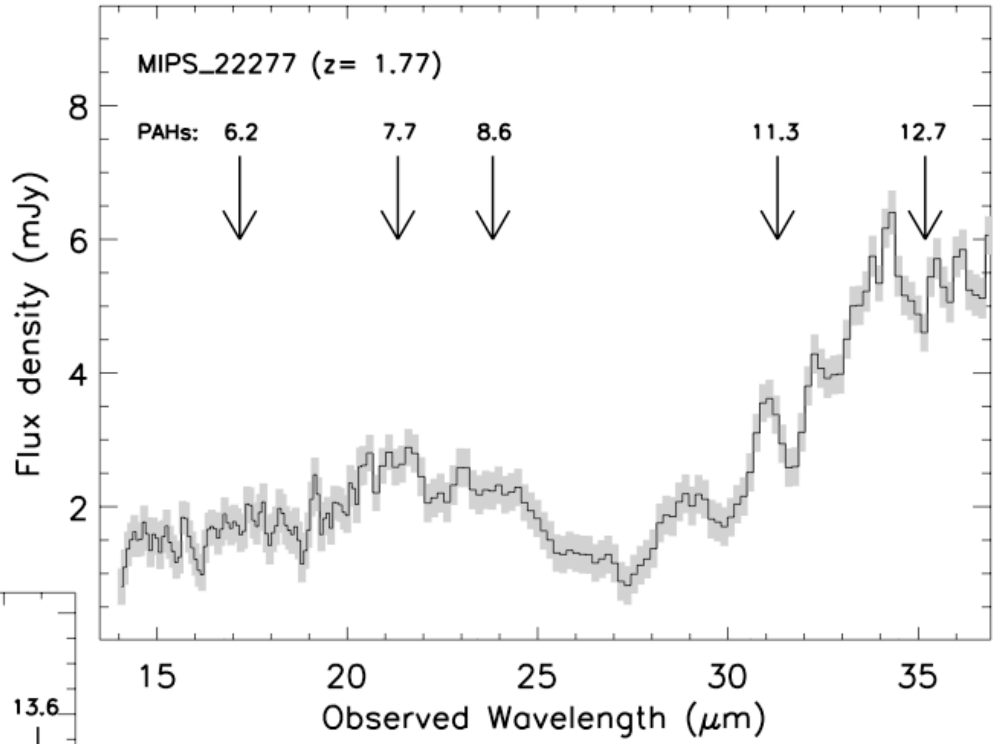
MIPS_22277 (z= 1.77)
PAHs: 6.2
7.7
8.6
11.3
12.7
Flux density (mJy)
Observed Wavelength (μm)

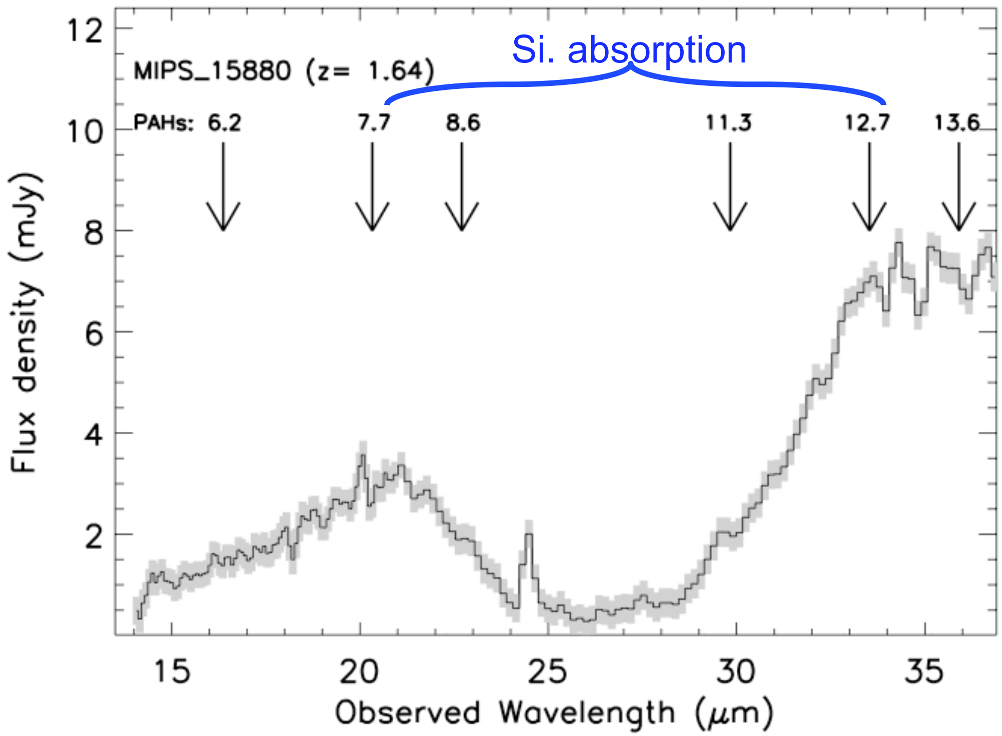
Si. absorption
MIPS_15880 (z= 1.64)
PAHs: 6.2
7.7
8.6
11.3
12.7
13.6
Flux density (mJy)
Observed Wavelength (μm)

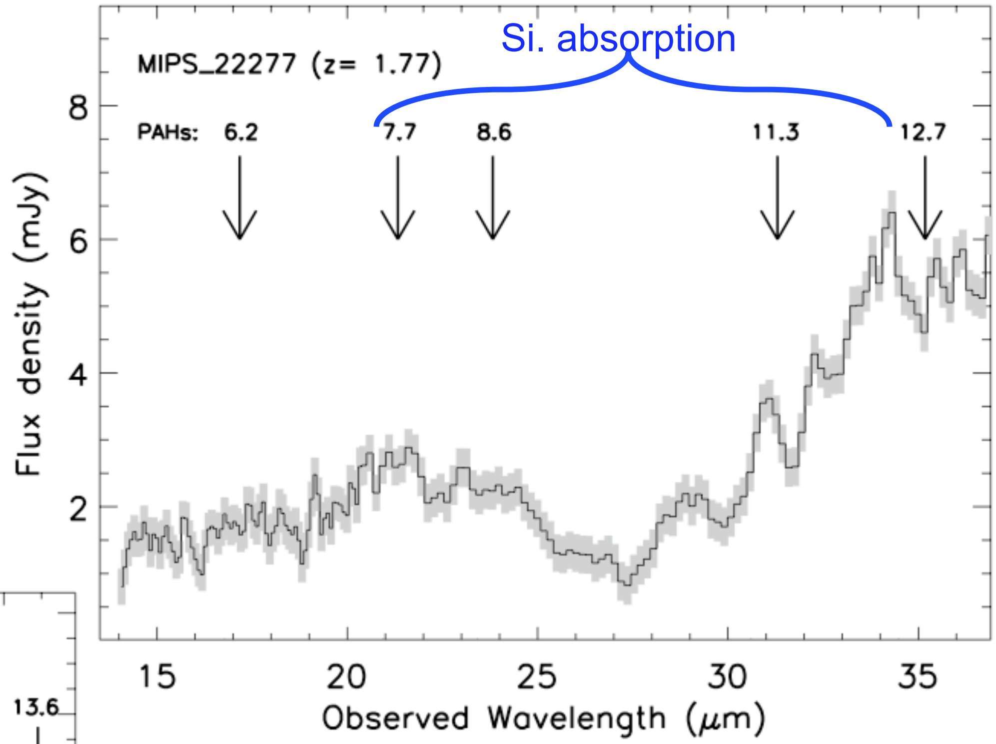
MIPS_22277 (z= 1.77)
Si. absorption
PAHs: 6.2
7.7
8.6
11.3
12.7
Flux density (mJy)
Observed Wavelength (μm)

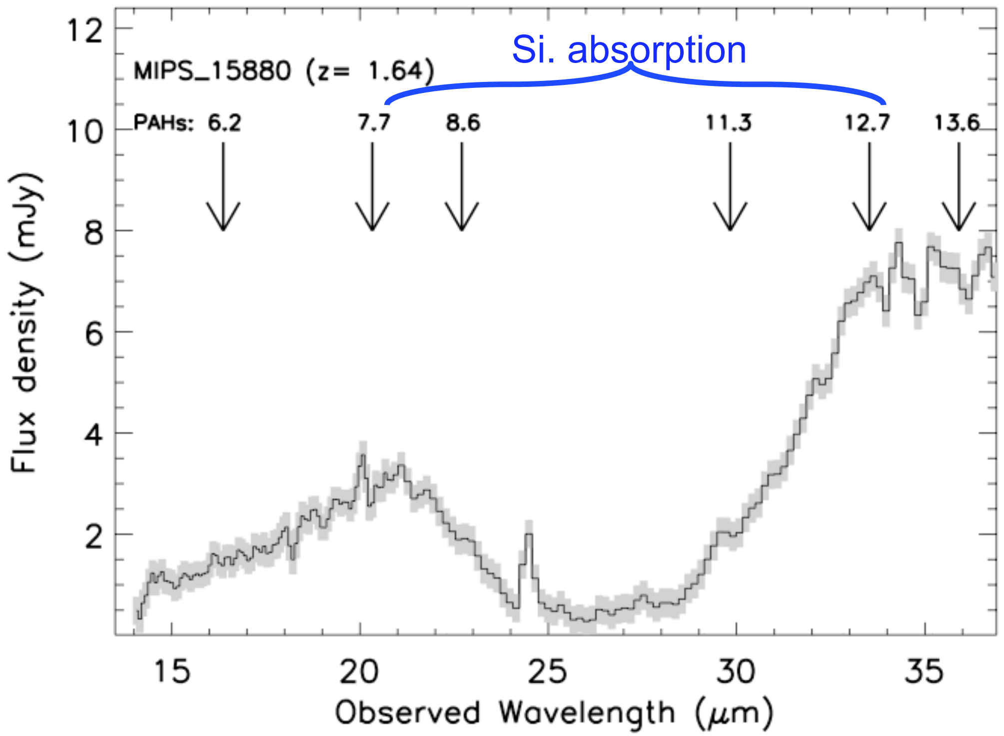
MIPS_15880 (z= 1.64)
Si. absorption
PAHs: 6.2
7.7
8.6
11.3
12.7
13.6
Flux density (mJy)
Observed Wavelength (μm)

Spectral results- stacking

Stacked spectrum of the high radio luminosity sample

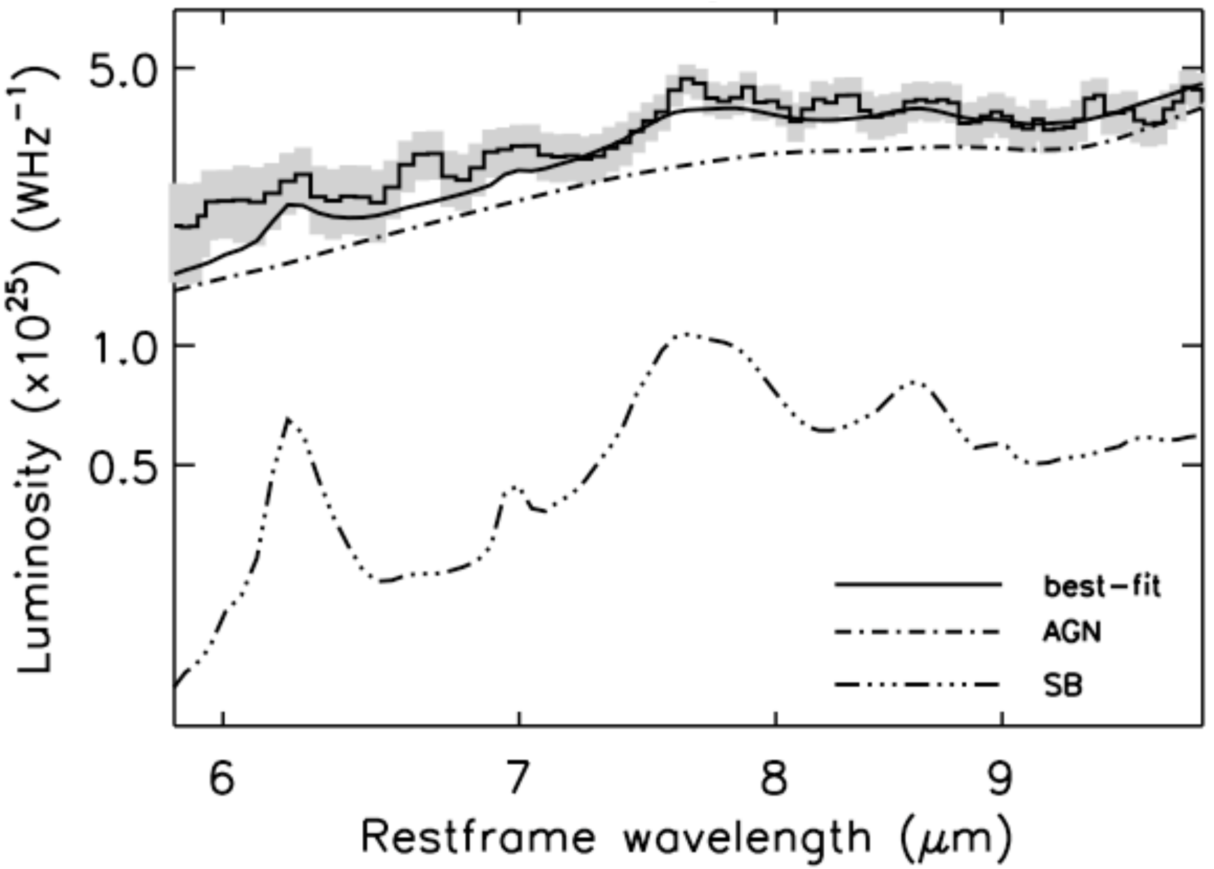

- Contribution from the SB component

Spectral results- stacking

Stacked spectrum of the high radio luminosity sample

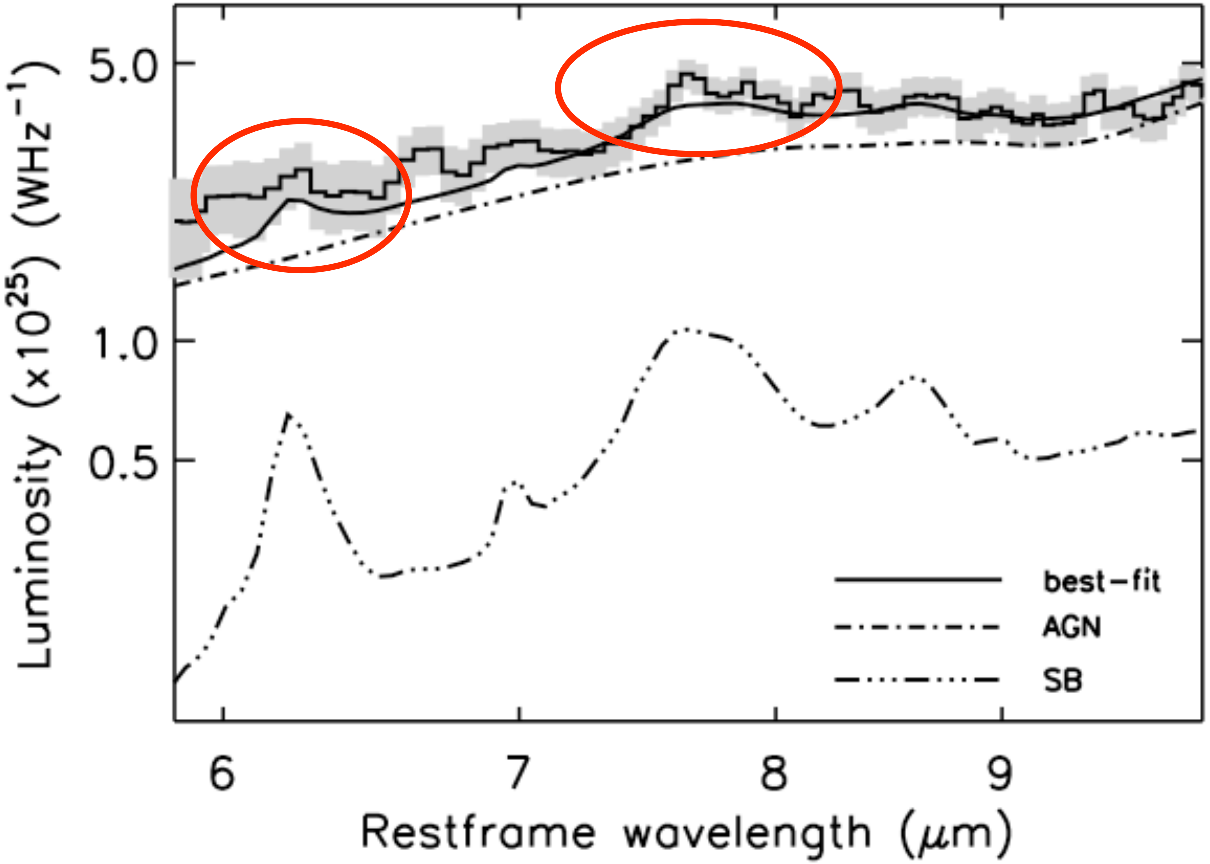

- Contribution from the SB component

Stacked spectrum of the moderate radio luminosity sample

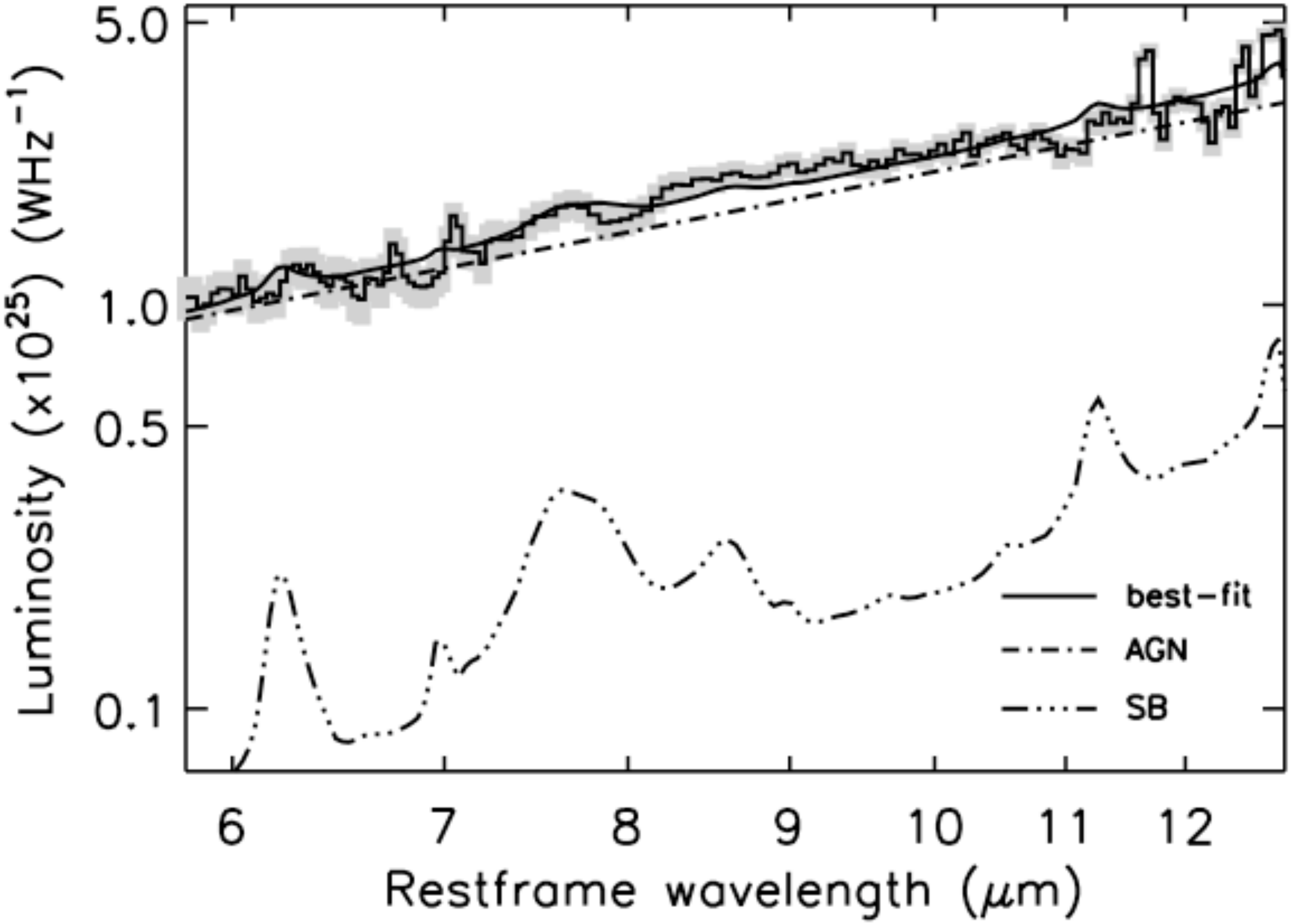

- Little contribution from the SB component

Stacked spectrum of the lower radio luminosity sample

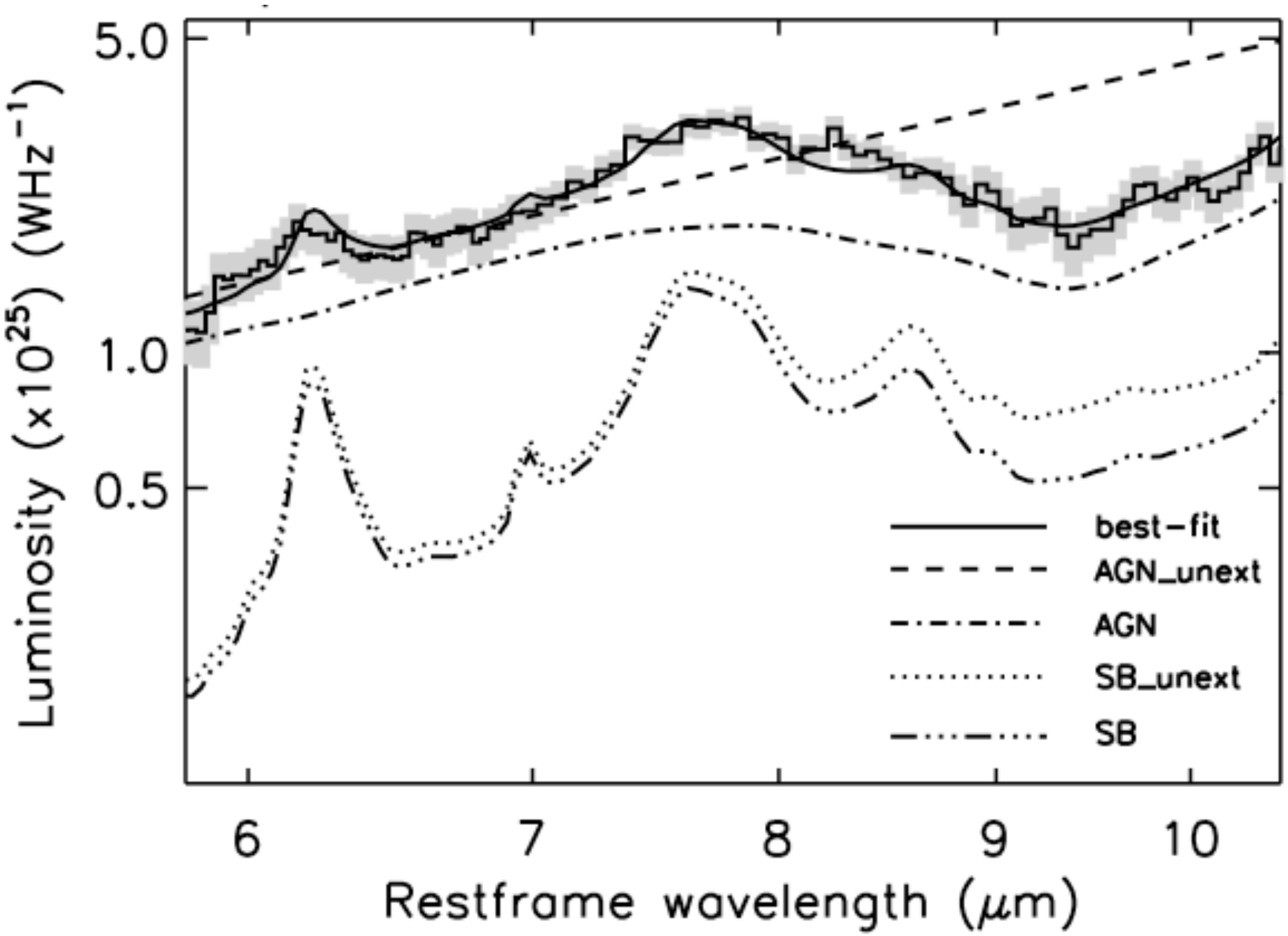

- Considerable contribution from the SB component

Stacked spectrum of the lower radio luminosity sample

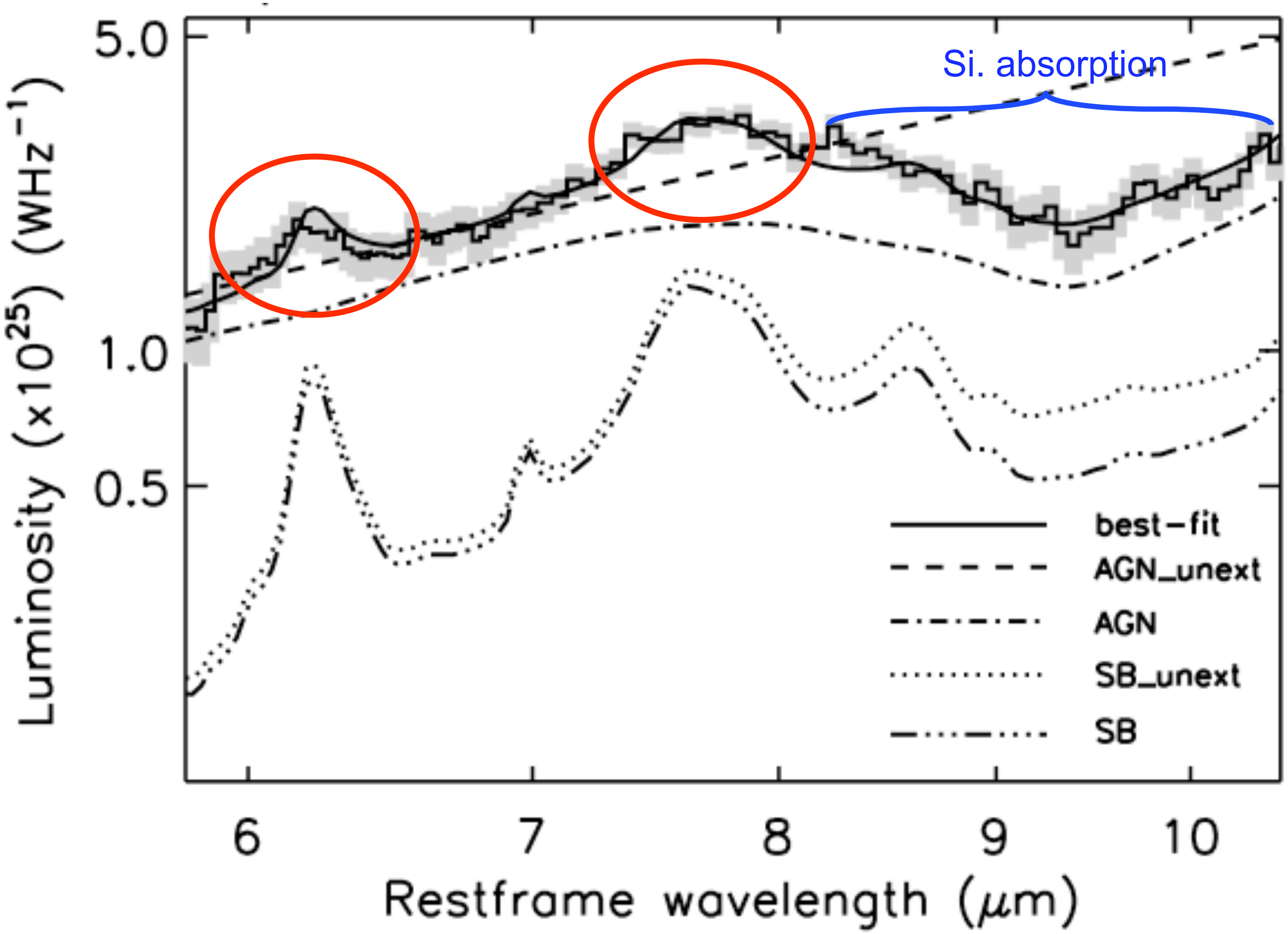

- Considerable contribution from the SB component

Preliminary stack results

- High luminosity:
  - PAH emission and weak silicate absorption
- Moderate luminosity:
  - Weak PAHs, no silicate absorption
- Lower luminosity:
  - Strong PAH emission and deep silicate absorption

- Unobscured SB -> PAH luminosities (6.2, 7.7 μm)

PAH luminosity- total IR luminosity correlation

- SMGs- Pope et al. 2008
- Local SBs- Brandl et al. 2006
- Kennicutt (1998):

  - Relation between total IR luminosity and SFR

SFR ($M_{sun}yr^{-1}$)

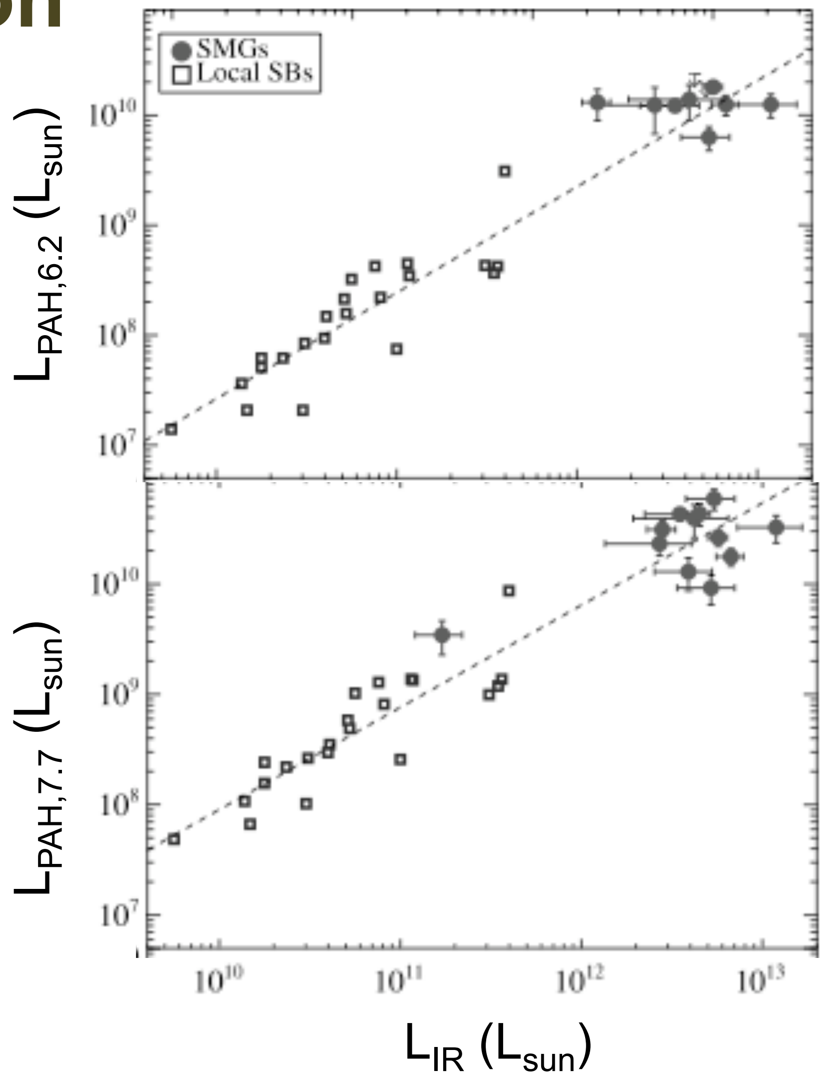

- High luminosity:

  - $L_{IR,7.7}$: ~10^{13} L_{sun}, $L_{IR,6.2}$: ~10^{13} L_{sun}

  - $SFR_{7.7}$: 1700 ± 600 $M_{sun}yr^{-1}$, $SFR_{6.2}$: 1700 ± 600 $M_{sun}yr^{-1}$

- Moderate luminosity:

  - $L_{IR,7.7}$: ~10^{12} L_{sun}, $L_{IR,6.2}$: ~10^{12} L_{sun}

  - $SFR_{7.7}$: 500 ± 400 $M_{sun}yr^{-1}$, $SFR_{6.2}$: 600 ± 500 $M_{sun}yr^{-1}$

- Lower luminosity:

  - $L_{IR,7.7}$: ~10^{13} L_{sun}, $L_{IR,6.2}$: ~ 10^{13} L_{sun}

  - $SFR_{7.7}$: 2200 ± 500 $M_{sun}yr^{-1}$, $SFR_{6.2}$: 2200 ± 500 $M_{sun}yr^{-1}$

Mid-IR luminosity traces AGN power

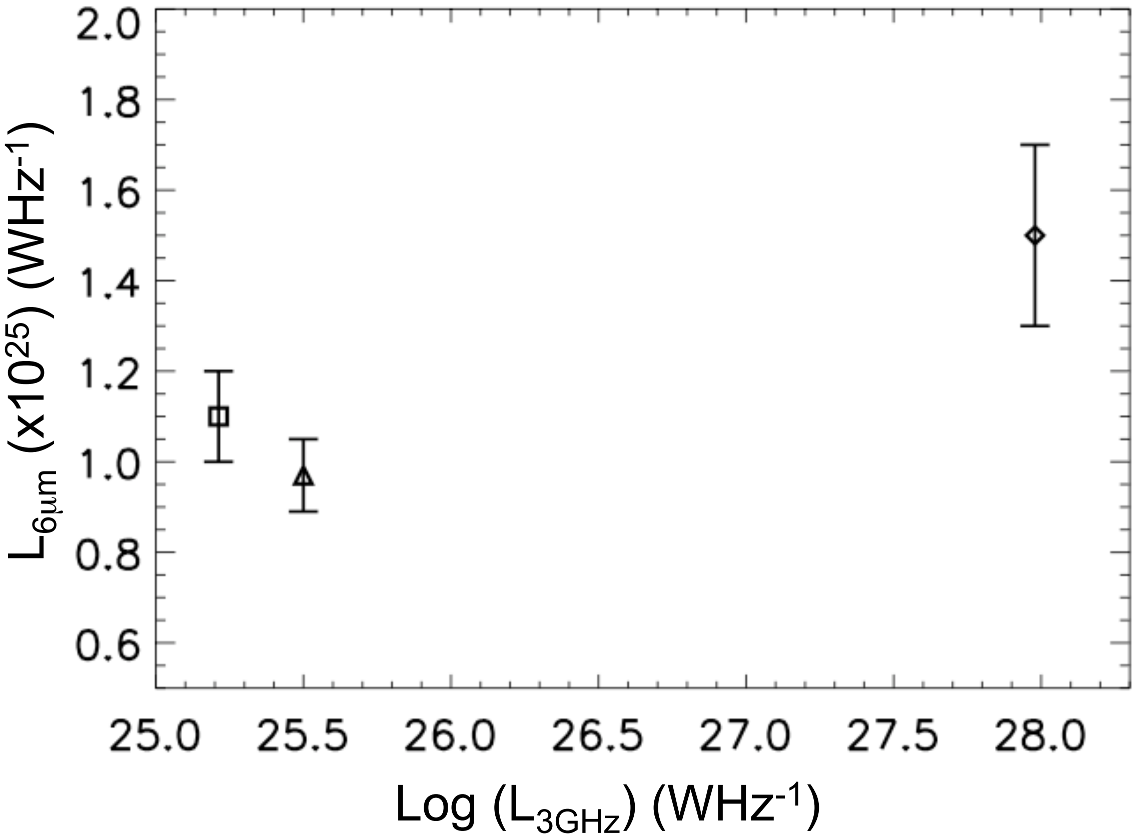

- Correlation between mid-IR - X-ray luminosities
  - Lutz et al. 2004
- Accretion rates and radio power- both properties of AGN

Feedback mechanisms taking place?

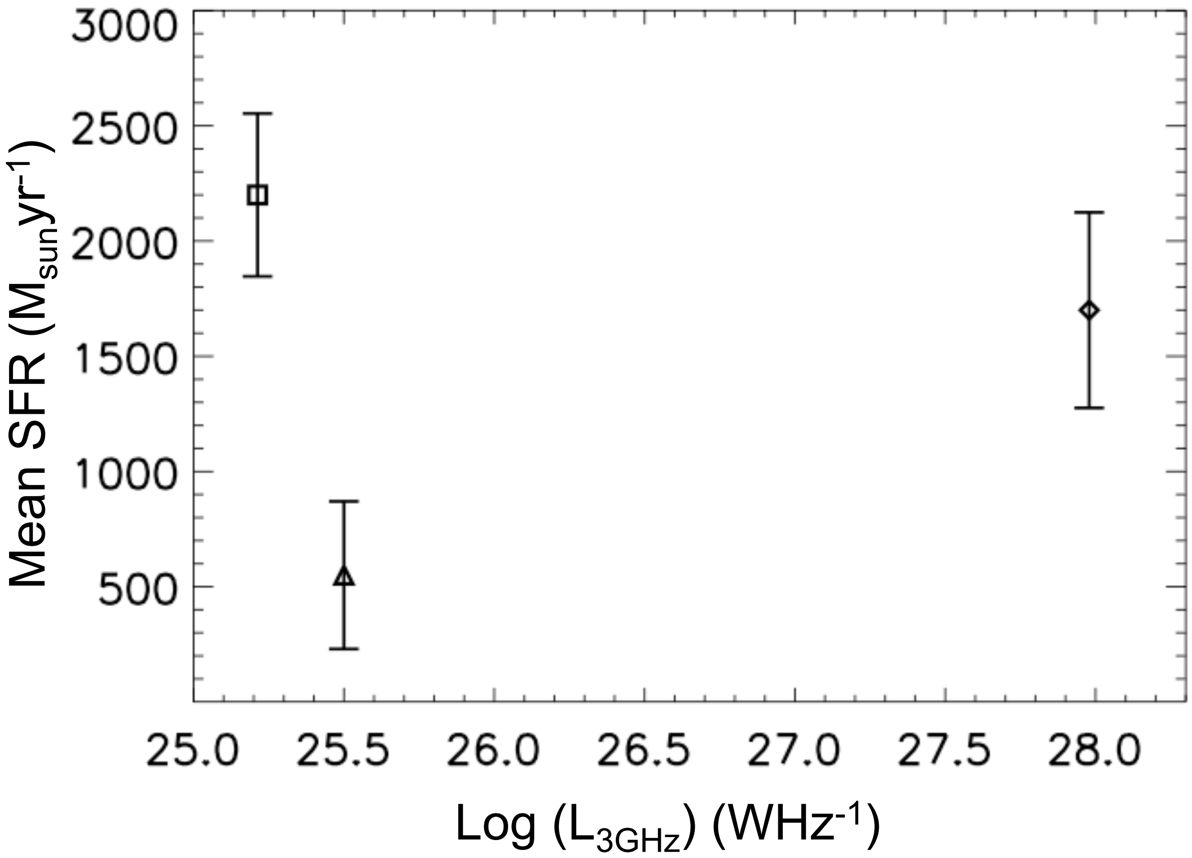

- No observed trend between SFRs and radio power

  - Before any potential feedback?

- No apparent connection between rate of growth of galaxy w.r.t. central black hole and radio power

- The greater the SB contribution the greater the galaxy growth w.r.t central black hole growth

- Fitting for individual spectra

Galaxy and black hole growth

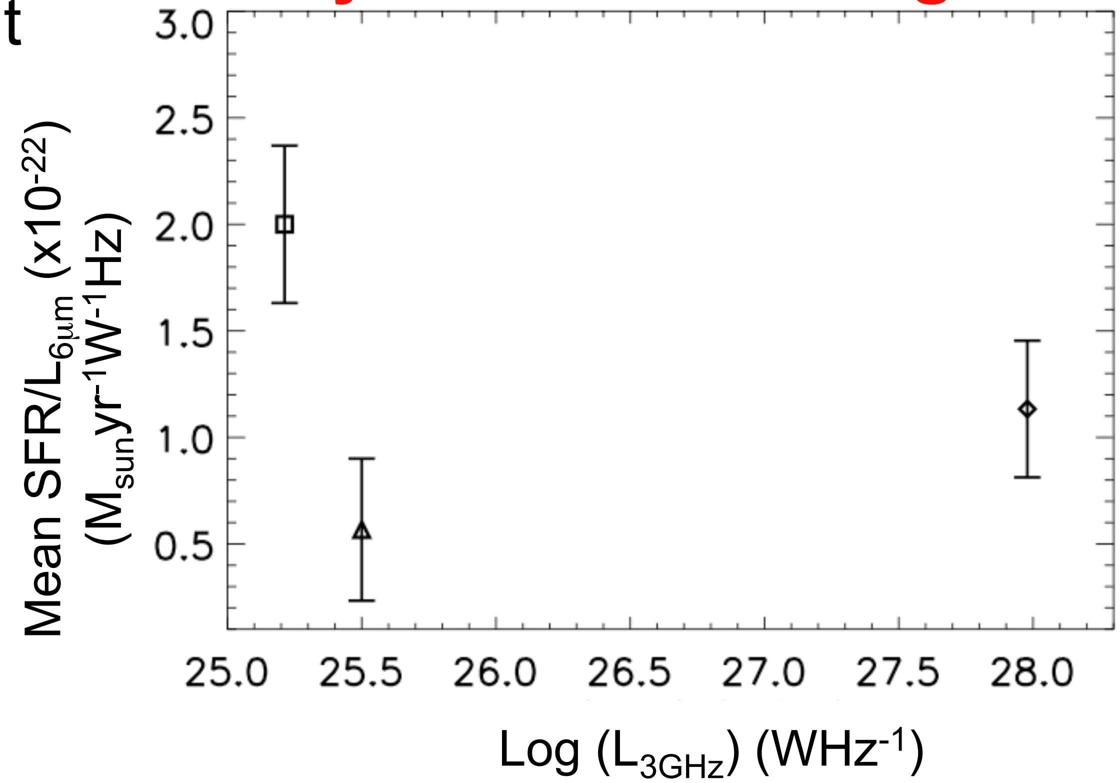

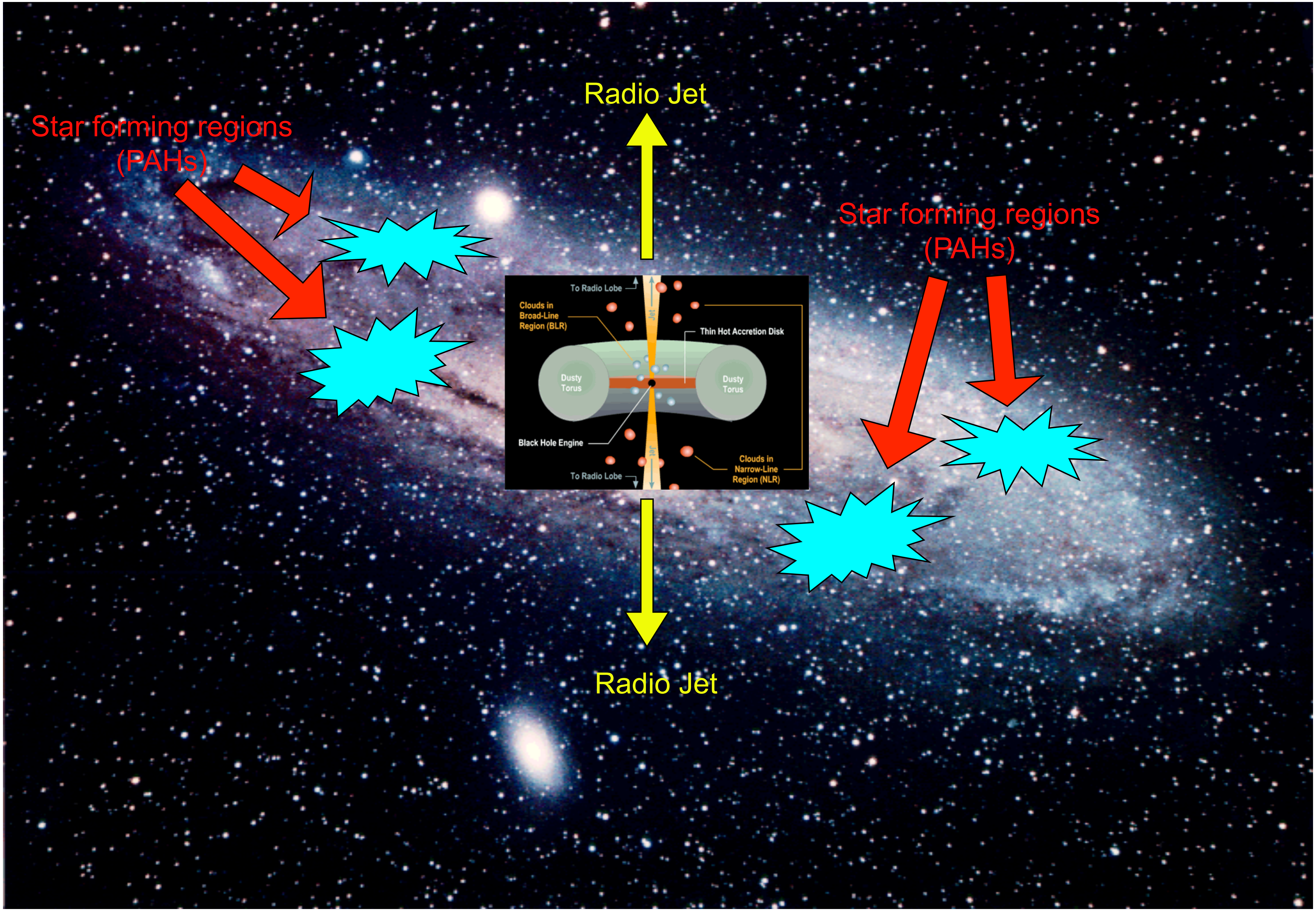
Radio Jet
Star forming regions
(PAHs)
Star forming regions
(PAHs)
To Radio Lobe
Clouds in
Broad-Line
Region (BLR)
Jet
Thin Hot Accretion Disk
Dusty
Torus
Dusty
Torus
Black Hole Engine
Jet
Clouds in
Narrow-Line
Region (NLR)
To Radio Lobe
Radio Jet

Conclusions

- Strong PAH emission observed at high redshift
- Powerful AGN, high SFRs and high total IR luminosities:
  - before feedback?
- High and lower luminosity samples:
  - Shielding of PAHs in some form
- Moderate luminosity sample:
  - Destroyed or weak
- Implied Coeval host galaxy and black hole growth
- Observing objects at a special time in their evolution

Rawlings et al. 2011 (in prep.)